electronic reprint

Acta Crystallographica Section B
Structural Science
ISSN 0108-7681

A novel perovskite-like Ta-bronze $KTa_{1+z}O_3$: preparation, stoichiometry, conductivity and crystal structure studies

Alla Arakcheeva, Gervais Chapuis, Vladimir Grinevitch and Vladimir Shamray

Acta Crystallographica Section B
Structural Science
ISSN 0108-7681

A novel perovskite-like Ta-bronze $KTa_{1+z}O_3$: preparation, stoichiometry, conductivity and crystal structure studies

Alla Arakcheeva,[a,b] Gervais Chapuis,[a]* Vladimir Grinevitch[b] and Vladimir Shamray[b]

[a]Institute of Crystallography, University of Lausanne, BSP, 1015 Lausanne, Switzerland, and [b]Baikov Institute of Metallurgy RAS, 117334 Moscow, Russia

Correspondence e-mail: email:gervais.chapuis@ic.unil.ch

Received 11 August 2000
Accepted 27 November 2000

A new cubic Ta-bronze (1) $KTa_{1+z}^{+(5-\delta)}O_3$ [$z \simeq 0.107$ (3)] was obtained on a cathode by molten salt electrolysis of the system K_2TaOF_5–$K_3TaO_2F_4$–$(KF + NaF + LiF)_{eutectic}$. Black, metallic cubic crystals of (1) are formed together with tetragonal β-Ta. The perovskite-like crystal structure of (1) [a = 4.005 (1) Å, space group $Pm\bar{3}m$] was refined with anharmonic displacement parameters for Ta and K atoms and anisotropic displacement parameters for a split O-atom position [KM4CCD diffractometer; λ(Mo $K\alpha$); 3320 measured reflections with $I > 3\sigma(I)$; R = 0.0095, wR = 0.0065, $\Delta\rho_{min}$ = −0.91 e Å^{-3}, $\Delta\rho_{max}$ = 0.65 e Å^{-3}]. Defects in the O and K atomic positions were found. (1) is a semiconductor in the temperature range 4–300 K, whereas the well studied and closely related colourless transparent crystals $KTa^{+5}O_3$ (2) are dielectric. Differences in the properties of (1) and (2) are assumed to be connected with the existence of Ta dumb-bells statistically distributed into the $KTaO_3$ matrix.

1. Introduction

Potassium tantalate, $KTaO_3$ (V), is a well known virtual ferroelectric that maintains its dielectric properties even down to 10 K (Geifman *et al.*, 1997). The perovskite-type crystal structure of the colourless transparent crystals $KTaO_3$ [space group $Pm\bar{3}m$; a = 3.9883 (2) Å] was studied with a high degree of precision (Zhurova *et al.*, 1992, 1995). The new cubic potassium tantalate, $K_xTa_{1+z}O_{3-y}$, which is presented here exhibits the same type of structure, but contains reduced $Ta^{5-\delta}$ ions.

In perovskite-type and relative compounds A_xBO_3 [A is an alkaline element, B is a transition metal (VI and V); $x < 1$], the reduction of the B element leads to unusual properties, such as an intense or metallic colour with metallic gloss, electric conductivity and other metal-like properties which are controlled by the stoichiometry of the compound. This family was named oxide bronze after A_xWO_3, which has been extensively studied (Cox, 1992). The metal-like appearance and electric conductivity of the newly obtained crystals suggest a new Ta oxide bronze.

In oxide bronze with the perovskite-type structure, the average oxidation number $(6 - x)$ of the cation located in the B site is between V and VI; the negative charge $(-x)$ of the BO_3 framework is compensated by an alkaline cation in the A position with partial occupation x. As an example, Na_xWO_3, where x = 0.54 and 0.73 (Wiseman & Dickens, 1976), belongs to this family. This traditional scheme of the perovskite-type structure is not valid for the new oxide bronze $KTa_{1+z}O_{3-y}$ owing to the reduced oxidation number of Ta, which is less than V. Crystal structure, electric conductivity and stoichiometry studies of this new cubic Ta-bronze are presented.

Table 1
Chemical composition of the new cubic Ta-bronze.

	Microprobe analyses		X-ray refinement results	
Chemical element	ARL-SEMQ % wt, % at	CAMEBAX % wt, % at	Anharmonic model (i) % wt, % at	Model with splitting of O positions (ii) % wt, % at
Ta	69.03 (65), 20.98	68.77 (72), 20.68	69.06, 21.02 (1)	68.29, 20.39 (1)
K	13.50 (13), 18.98	13.36 (51), 18.58	13.54, 19.07 (1)	13.78, 19.05 (1)
O	17.47 (58), 60.94	17.87 (65), 60.75	17.40, 59.91 (2)	17.93, 60.56 (2)
F	< 0.02, –	–	–	–
Nb	< 0.01, –	–	–	–
Total	100, 100	100, 100	100, 100	100, 100
Chemical composition	$K_{0.905\ (40)}TaO_{2.86\ (8)}$	$K_{0.898\ (60)}TaO_{2.94\ (9)}$	$K_{0.907\ (3)}TaO_{2.86\ (3)}$	$K_{0.934\ (1)}TaO_{2.974\ (3)}$

2. Experimental

2.1. Synthesis

The metallic and cubic-shaped black crystals, together with the light grey dendrite-like metallic formation (Fig. 1) did grow on a cathode during the electrolysis of oxofluoride–fluoride melts with metallic Ta or TaO soluble anodes. K_2TaOF_5 or $K_3TaO_2F_4$ were used as a Ta-containing component for the electrolyte. The ternary eutectic LiF–NaF–KF was used as a solvent. The electrolysis was carried out in the potential static mode with temperature ranging from 923 to 1023 K and a cathode current density of 0.1–0.3 A cm^{-2} in an atmosphere of high-purity argon. The electrolytic cell consisted of a glassy carbon crucible containing 50 g of molten electrolyte. The anode material was located on the bottom of the crucible. The Mo cylindrical cathode was placed in the centre of the cell. After completion of the electrolysis cycle, the cathodic rod and its deposit was cooled in the water chamber placed in an argon atmosphere. Finally, the cathode product was washed free of the entrapped salt phase, first with hot 20% HCl acid and then in distilled water and ethanol. A thin film formed on the surface of the molten electrolyte in contact with the cathode is also among the cathode products.

An X-ray powder diffraction study [DRON-3M diffractometer, Cu $K\alpha$ radiation] reveals the existence of two phases at the cathode. The black metallic well-shaped cubic crystals and the thin film belong to a perovskite-like phase with the unit-cell parameter a = 4.00 (1) Å. The dendrite-like formations with a light grey metallic colour are the tetragonal β-Ta phase with the unit-cell parameters a = 10.19 (1) and c = 5.31 (1) Å (JCPDS-ICDD PDF-2 database, No. 25-1280 after Moseley & Seabrook, 1973). The ratio between the two phases varies approximately from 10:1 to 1:1. Note that the electrolytic crystallization of the perovskite-like phase on the cathode is a manifestation of its electric conductivity.

The perovskite-like phase was also heated in air for 1 h at 1093 K. In this experiment, the black cubic crystals turn white and the X-ray powder diffraction patterns exhibit the same perovskite-like structure.

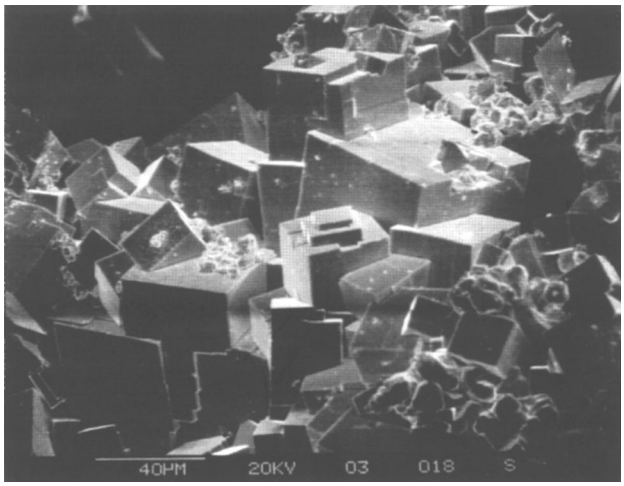

Figure 1
Crystals of $KTa_{1+z}O_3$ obtained by electrolytic crystallization.

2.2. Electron microprobe study

The two detected phases were studied using the microprobe analyser ARL-SEMQ (15 kV, 25 nA) with EDAX (12 kV, 100 nA). The size of the crystal cubes of the new perovskite-like phase (Fig. 1) varies from 5 to 100 μm. No trace of Li and Na elements could be detected in the sample. The metallic α-Ta (Ta, $L\alpha$), the mineral orthoclase (K, K_α), LiF crystal (F, $K\alpha$) and metallic Nb (Nb, $L\alpha$) were used as standards for the quantitative analysis of the chemical composition. All the standard corrections have been applied for the calculation of the element concentrations. Only 5–10% wt Nb was found as an impurity in the β-Ta phase. In the cubic crystals of the new perovskite-like phase, three different morphological zones have been examined. The first zone is the well-shaped cubic face (100). The second zone is an irregular crystal surface. The third zone is the cubic (100) face with a small formation of the β-Ta on its surface. Microprobe analyses obtained from all three zones showed practically the same chemical composition for this new perovskite-like cubic crystal. It should be mentioned that less than 0.2% wt F was detected in the thin superficial layers and an order of magnitude less below the surface of the cubic crystals. According to the present investigation (Table 1), the average of the composition for the new perovskite-like phase corresponds to the formula $K_{0.91}Ta_{1.10}O_{3.14}$. This composition was confirmed by the data obtained for this phase with the CAMECA microprobe analyser using $KTaO_3$ as standard. These results are in good agreement with the crystal structure refinement of the present work (Table 1). The generalization of these data leads to the chemical formula $K_{1.00\ (2)}Ta_{1.10\ (3)}^{+(5-\delta)}O_{3.14\ (12)}$, where δ = 0.15 (8). This phase may be represented as $KTa_{1+z}O_3$ with some comments indicated below.

2.3. Electric conductivity study

The temperature dependence of the electrical conductivity in the range 4.2–300 K has been studied by the four-contacts method of measurement using films of the new perovskite-like phase with ~0.2 mm^2 in cross section and ~1.5 mm in length. The measuring current was 10^{-4} A. The electric resistivity (Fig. 2) of the specimens exhibit a semiconductor type of temperature dependence. Therefore, the new black-metallic phase $K_xTaO_{3-y}KTa_{1+z}O_3$ with reduced Ta ions can be considered as a cubic Ta-bronze (1) in contrast with the well known dielectric transparent crystals $KTa^{5+}O_3$ (2).

Crystals (1) and (2) belong to the same perovskite-like structure type. Differences in their structural features are of immediate interest in order to explain the differences in their physical properties. Structure, electron density and thermal vibration of the atoms were studied for (2) by X-ray single-crystal diffraction (Zhurova *et al.*, 1992, 1995). In our study we used the same method for comparison purposes.

2.4. X-ray measurements

Details of the crystal data and data collection for crystal (1) are given in Table 2. The KM4CCD diffractometer was operated with tube voltage 55 kV and filament current 45 mA. The crystal–detector distance of 51.4 mm was set for the measurements, including high-angle reflections. The experimental data were obtained in the dynamic scanning mode. The unit-cell parameter a was refined from $K\alpha_1$ peaks. The integrated intensities were corrected for Lorentz, polarization and absorption effects. The program *Movie* (Oxford Diffraction Ltd, 2001) was used to measure the shape of the crystal for the absorption correction. The diffraction pattern of the analysed sample appeared to be of very high quality. No diffuse scattering could be observed.

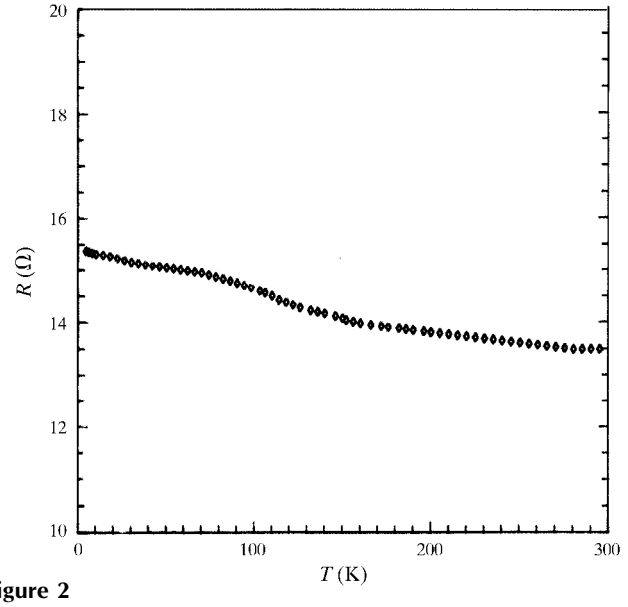

Figure 2
Temperature dependence of the resistivity for $KTa_{1+z}O_3$.

Table 2
Experimental details.

Crystal data		
Chemical formula	$K_{0.934}O_{2.94}Ta$	
Chemical formula weight	264.5	
Cell setting, space group	Cubic, $Pm\bar{3}m$	
a, b, c (Å)	4.0050 (4), 4.0050 (4), 4.0050 (4)	
α, β, γ (°)	90.00 (1), 90.00 (1), 90.00 (1)	
V (Å^3)	64.240 (11)	
Z	1	
D_x (Mg m^{-3})	6.835	
Radiation type	Mo $K\alpha$	
No. of reflections for cell parameters	3320	
θ range (°)	5.08–71.04	
μ (mm^{-1})	43.966	
Temperature (K)	295	
Crystal form, colour	Box, black metallic	
Crystal size (mm)	0.054 × 0.050 × 0.030	
Data collection		
Diffractometer	KM4	
Data collection method	CCD scans	
Absorption correction	Gaussian integration	
T_{min}	0.290	
T_{max}	0.770	
No. of measured, independent and observed parameters	3320, 148, 148	
R_{int}	0.0252	
θ_{max} (°)	71.33	
Range of h, k, l	$-10 \rightarrow h \rightarrow 10$ $-9 \rightarrow k \rightarrow 10$ $-10 \rightarrow l \rightarrow 8$	
Refinement		
Refinement on	F	
$F(000)$	113	
R [148F with sin $\theta/\lambda < 1.27$]	0.0096	0.0094
wR	0.0079	0.0060
S	3.25	3.05
No. of reflections and parameters used in refinement	168, 26	168, 16
Weighting scheme	$w = 1/\sigma^2(F)$	
$(\Delta/\sigma)_{max}$	0.0139	
$\Delta\rho_{max}$, $\Delta\rho_{min}$ (e Å^{-3})	0.91, −1.56	0.82, −0.86
Extinction method	Becker–Coppens; type 1; Gaussian distribution	
Extinction coefficient	0.0127 (2)	0.0149 (2)

† Computer programs used: *JANA*2000 (Petrícek & Dusek, 2000*a*,*b*).

3. Structure refinement and results

The refinement of the crystal structure of (1) was adapted to the refinement procedures used for (2) (Zhurova *et al.*, 1992, 1995). The characteristics of the procedures are listed in Table 2.[1] Neutral atomic scattering factors were applied. The anomalous scattering effect was duly accounted for. The scaling factor, extinction and occupancy parameters of the K and O atoms were determined using the whole set of averaged reflections (168 intensities). The atomic displacement tensors were refined from high-angle data in the range $0.7 < \sin\theta/\lambda < 1.35$. The correlated parameters were refined separately by successive alternation using a low value of the damping factor. Since only 148 independent reflections with $\sin\theta/\lambda < 1.27$ were

[1] Supplementary data for this paper are available from the IUCr electronic archives (Reference: OS0066). Services for accessing these data are described at the back of the journal.

used for the structure calculations of (2), all our refinements were performed with this subset of reflections as well. All the atomic parameters obtained with both sets of 168 and 148 reflections were practically the same. For comparison, the atomic parameters listed in Table 3 correspond to the refinement with 148 reflections ($\sin\theta/\lambda < 1.27$). The deformation electron density (DED) function was also calculated [$\delta\rho = \rho_e - \rho_{cr}$, where ρ_e is the experimental electron density and ρ_{cr} is the electron density calculated with high-angle reflections ($\sin\theta/\lambda > 0.7$) and with isotropic thermal displacements].

The refinement was performed for three models of atomic thermal atomic displacements:

(i) anharmonic displacements for all atoms;

(ii) anharmonic displacements of Ta and K atoms and anisotropic displacements of the split O atomic position;

(iii) anisotropic displacements of split atomic positions for all the atoms.

Physically meaningful results with positive atomic temperature factors were obtained only for models (i) and (ii) (Table 3). The optimization parameters and the results obtained seem to be realistic for both models (Table 2 and 3). The R factors are practically identical. The number of parameters refined, the values of the extrema $\Delta\rho$ and GOF are smaller for model (ii), but the temperature factor U^{11} for the O atom is practically zero, which might indicate the higher value of its population factor in comparison to the microprobe data (Table 1). The anharmonic refinement (i) is characterized by reasonable displacement parameters of the O atom and a stoichiometry of (1) very close to the microprobe results (Table 1). Since the difference between (i) and (ii) lies in the modelling of thermal displacements of the O atom only, namely strong anharmonic vibration (i) or splitting (ii) of its position along the [100] direction, it can be concluded that the O atom at least tends to have a split position along this direction (Ta–O line). As seen from the values of the anharmonic tensors (Table 2), this tendency is much more pronounced in (1) than in (2). This conclusion is confirmed by the probability density function (PDF) calculated for the O atom (Fig. 3*a*) with the parameters obtained in model (i). This function has physically meaningless regions of negative values in the vicinity of the point ($\frac{1}{2}$, 0, 0) and two maxima at (0.516, 0, 0) and (0.484, 0, 0), which correspond to the split position of O in model (ii). Similar results were obtained for crystal (2) (Zhurova *et al.*, 1995) as well. In (1) the PDF of Ta atoms have only one maximum (0, 0, 0) slightly extended along the (100) and (010) directions (Fig. 3*b*), while (2) has maxima spherically distributed around the origin with a physically meaningless negative minimum at the centre (Zhurova *et al.*, 1995). The PDF of the K atom (Fig. 3*c*) has only one maximum both in (1) and (2).

4. Discussion

The main goal of the present study is to reveal the differences in the crystal structures and the stoichiometry between the semiconductor phase (1) ($KTa_{1+z}O_3$ or K_xTaO_{3-y}) and the isolator phase (2) ($KTaO_3$), which differ greatly in their physical properties. The heating experiment with the colour change described above confirms the lower oxidation state of Ta in (1), as compared with Ta^{+5} in (2).

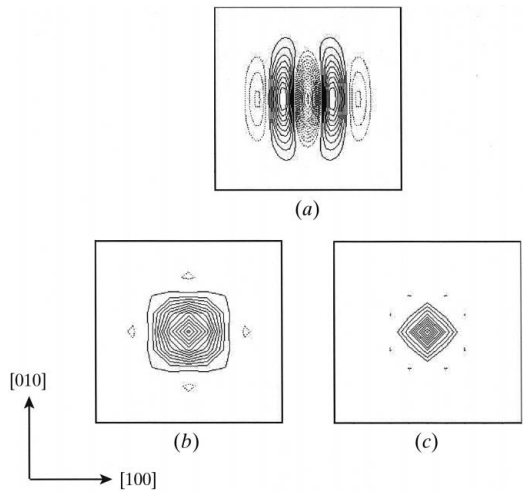

Figure 3
The (001) section of the PDF maps for (*a*) O, (*b*) Ta and (*c*) K atoms calculated for the anharmonic model of the atomic displacements in $KTa_{1+z}O_3$. Contour intervals at 500 Å^{-3}. The framework dimension is 0.5 Å.

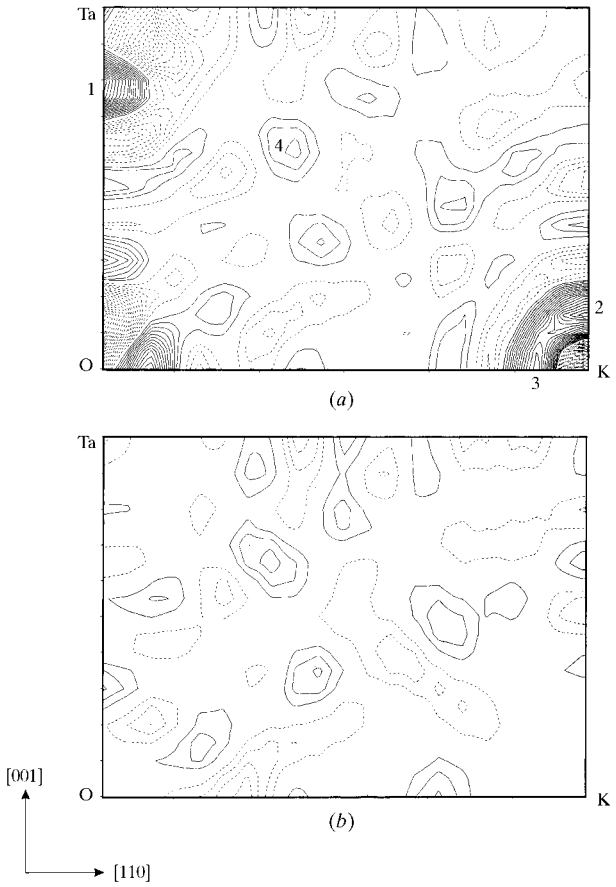

Figure 4
Maps of (*a*) deformation electron density and (*b*) residual electron density in the (110) plane for $KTa_{1+z}O_3$ calculated on the basis of 148 reflections with $\sin\theta/\lambda < 1.27$. Contour intervals are at 0.2 e Å^{-3}. The numbers indicate important maxima discussed in the text.

Table 3
The results of $KTa_{1+z}O_3$ structure refinement in comparison with $KTaO_3$.

	$KTa_{1+z}O_3$ (present work)		$KTaO_3$ (Zhurova *et al.*, 1995)	
Parameters	Anharmonic model (i)	Model with split O position (ii)	Anharmonic model	Model with split O and Ta positions
K				
p	0.907 (3)	0.959 (1)	1	1
$x = y = z$	0.5	0.5	0.5	0.5
U (Å^2)	0.0013 (2)	0.0042 (2)	0.0077 (1)	0.00783 (4)
D1111 × 10^4	−0.029 (2)	−0.017 (2)	0.0001 (2)	–
D1122 × 10^4	−0.0063 (9)	−0.0038 (9)	0.0001 (9)	–
F111111 × 10^6	−0.018 (2)	−0.010 (2)	–	–
F112233 × 10^6	−0.0004 (2)	−0.0002 (2)	–	–
F111122 × 10^6	−0.0023 (3)	−0.0013 (3)	–	–
Ta				
$x = y = z$	0	0	0	0.0117 (4)
U (Å^2)	0.0057 (1)	0.0065 (1)	0.00337 (3)	0.0020 (2)
D1111 × 10^4	−0.0009 (9)	0.0024 (8)	−0.00093 (3)	–
D1122 × 10^4	−0.0011 (3)	−0.0008 (2)	−0.00028 (1)	–
F111111 × 10^6	−0.0011 (6)	0.0005 (5)	–	–
F112233 × 10^6	−0.00019 (6)	−0.00022 (5)	–	–
F111122 × 10^6	−0.0003 (1)	−0.00021 (8)	–	–
O				
p	0.95 (1)	0.98 (1)	1	1
x	0.5	0.515 (1)	0.5	0.514 (5)
$y = z$	0	0	0	0
U^{11} (Å^2)	0.003 (1)	0.0009 (3)	0.0037 (5)	0.001 (3)
U^{22} (Å^2)	0.0050 (8)	0.0078 (2)	0.0075 (4)	0.0081 (1)
D1111 × 10^4	0.03 (1)	–	−0.0005 (9)	–
D2222 × 10^4	−0.015 (7)	–	−0.0006 (6)	–
D1122 × 10^4	−0.002 (3)	–	−0.0002 (2)	–
D2233 × 10^4	0.008 (5)	–	0.0000 (3)	–
F111111 × 10^6	−0.011 (3)	–	–	–
F111122 × 10^6	0.0003 (1)	–	–	–
F111133 × 10^6	0.003 (1)	–	–	–
F112222 × 10^6	−0.0003 (3)	–	–	–
F112233 × 10^6	0.0005 (3)	–	–	–
F222222 × 10^6	0.031 (2)	–	–	–

The atomic parameters of (1) and (2) do not reveal any qualitative difference, except for the vacancies in the K and O positions in (1). Measurement at different temperatures are required to give a preference to the split or anharmonic model both for (1) and (2). At this point, a comparative analysis of the DED function for both compounds is of interest. The main features of the DED functions for (1) (Fig. 4*a*) and (2) (Zhurova *et al.*, 1995) are similar: the high positive peaks are localized on the T—O and K—O lines, but strongly shifted towards oxygen in K—O. Taking into account the uncertainty of the DED function interpretation for crystals containing heavy atoms, especially with anharmonic thermal displacements (Restori & Schwarzenbach, 1996), we restrict our comparison of (1) and (2) to the essential differences in their DED functions. A few additional maxima can be found in (1). High positive maxima are observed near Ta and K with distances from both cations of ∼0.64–0.85 Å in the [100] direction (1 and 2 on Fig. 4*a*, respectively) and ∼0.6 Å in the [110] direction from K (3 on Fig. 4*a*). These maxima are parameterized by the anharmonic tensors of K and Ta and are absent on the residual map (Fig. 4*b*). Their absence on the map for structure (2) confirms the weaker anharmonic displacement of K and Ta atoms in (2) (Table 3). The maximum ∼0.6 e Å^{-3} is ∼1.3 Å distant from Ta in the [111] direction (4 on Fig. 4*a*). This maximum subsists on the residual map (Fig. 4*b*) and is usually associated with $t_{2g}(5d)$ Ta orbitals. It is absent on the map corresponding to (2). Another maximum is observed on the residual map at (0.5, 0.5, ∼0.16). Its height is ∼0.4 e Å^{-3} and it is ∼1.4 and 2.9 Å distant from K and Ta, respectively. This is the highest maximum on the residual map calculated with 168 independent reflections (crosses on Fig. 5). The points of the crystallographic site 6(*f*): ($\frac{1}{2}$, $\frac{1}{2}$, z = 0.16) form an octahedron with 1.4 Å distances from the center position ($\frac{1}{2}$, $\frac{1}{2}$, $\frac{1}{2}$) occupied by K (Fig. 5). This centre can be interpreted as a crossing of three dumbbells of Ta atoms distant by 2.8 Å (Fig. 6). Such a Ta—Ta distance is characteristic of both α-Ta and β-Ta modifications. Taking into account that the doping M^+ ion usually occupies this crystallographic position in $K_{1-x}M_xTaO_3$ [for example, Li in 6(*f*): (0.5, 0.5, z = 0.09); Zhurova *et al.*, 1992], we postulate the presence of a small amount of Ta atoms in this position. Owing to the very small density of this position, the refinement of this atomic position yields a population parameter of the same order of its accuracy.

Summarizing our results on the stoichiometry study of (1) (K_xTaO_{3-y}), we observe that the ratio K/Ta is less than 1 and the ratio O/Ta is less than 3. For the crystal under study, the estimated values are x = 0.91 (2) and y = 0.1285 (7). The nominal oxidation state of the Ta atoms is +4.85 (8) in the semiconductor (1) in contrast with +5 for the insulator (2). Thus, the additional electrons characterize the semiconductor phase (1) in comparison to the insulator phase (2). Therefore, it can be concluded that the increase of the electrical conductivity in (1) is similar to what is usually observed in a semiconductor produced by doping an insulator. In a first stage, when the doping is relatively small, impurity states arise. By increasing the doping concentration, the formation of an impurity zone takes place. As a result, a transition from insulator to metal could occur in this system. On the other hand, doping $KTaO_3$ with Fe^{+3} results in oxygen vacancies, forming dipole defects and does not lead to the insulator-semiconductor transition nor to the metallic colour of the crystals (Geifman & Golovina, 1994).

On the basis of our results, we propose the following explanation. The populations of K and O positions are prac-

tically the same in crystal (1) (Table 3). This is in accordance with the existence of Ta–Ta dumb-bells distant by approximately 2.8–2.9 Å statistically distributed in the crystalline $KTaO_3$ matrix of (1) around vacant K positions. It should be mentioned that the octahedral configuration of the Ta positions is only the result of a time or space average. Only one of the three possible dumb-bell positions can be present at any site. In the octahedron cluster, the distance between nearest atoms is ~1 Å, which excludes simultaneous occurrence. The dumb-bell may align along [001], [010] or [001] each with 1/3 population according to the symmetry requirement. The [Ta_6] cluster is represented in Fig. 6. In other words, the regular structure of crystal (1) is characterized by deficient K and O positions, which can be statistically substituted by Ta–Ta dumb-bells. These additional Ta atoms form specific coherent defects in the regular crystal structure (1). The conventional formula of (1) should be expressed as [$KTaO_3$ + Ta_z] or $KTa_{1+z}O_3$ [$z \simeq 0.107\,(23)$]. Notice that the simultaneous presence of the O atoms in the regular structure surrounding Ta in the dumb-bell positions is possible because the shortest Ta—O distance is larger than 2 Å. The structural data obtained for the regular structure of (1) are very close to those of (2). Therefore, it can be concluded that the structure of the main matrix $KTaO_3$ is practically independent from the existence of Ta dumb-bells partially substituted with K atoms. Crystals of (1) exhibit a weak dependence of the electrical resistivity on the temperature-independent minimum of the metallic conductivity usually of the order of $\sigma \simeq 100\ \Omega^{-1}\ cm^{-1}$ (Mott & Devis, 1979). Therefore, it cannot be excluded that the conductivity of the phase $KTa_{1+z}^{+(5-\delta)}O_3$ is close to this limit.

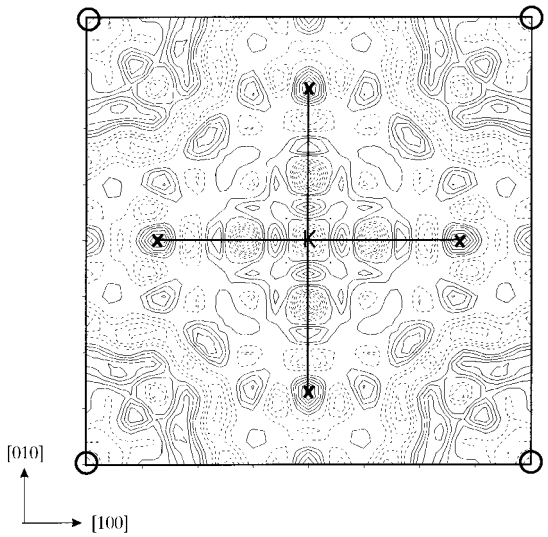

Figure 5
Residual electron density of the (001) section on the basis of 168 reflections with $\sin\theta/\lambda < 1.27$. Potassium (K) is at the centre and O atoms are on the vertices of the map. Crosses point to the highest maxima associated with the Ta dumb-bells indicated by solid lines in the $KTaO_3$ matrix of $KTa_{1+z}O_3$.

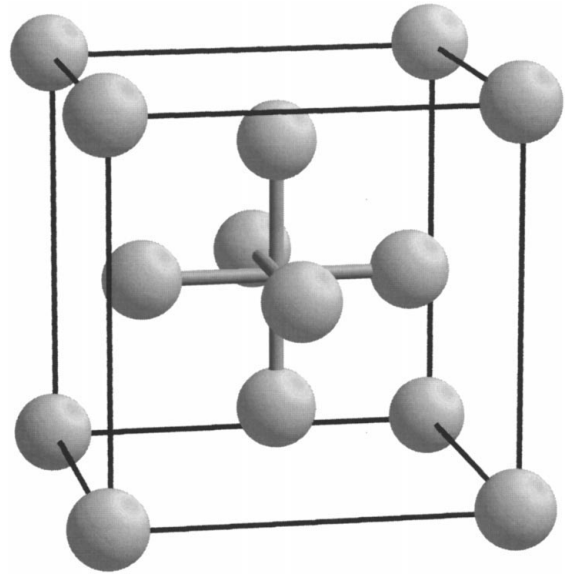

Figure 6
[Ta_6] cluster statistically occupied by a Ta_2 dumb-bell in three orientations.

The microprobe analyses of G. Burri (CMA, University of Lausanne), M. Kantor (Baykov Institute of Metallurgy, Moscow) and the electrical conductivity measurement of V. Mitin (Kapitza Institute, Moscow) are gratefully acknowledged. One of the authors (AA) is grateful to the Herbette Foundation of the University of Lausanne for financial support. VG and VS are grateful to the Russian Fundamental Scientific Foundation (grant No. 32804).

References

Cox, P. A. (1992). *Transition Metal Oxides: An Introduction to their Electronic Structure and Properties*. Oxford: Clarendon Press.
Geifman, I. N. & Golovina, I. S. (1994). *Crystallogr. Rep.* **39**, 57–60.
Geifman, I. N., Golovina, I. S. & Son'ko, T. V. (1997). *Crystallogr. Rep.* **42**, 428–431.
Moseley, P. T. & Seabrook, C. J. (1973). *Acta Cryst.* B**29**, 1170–1171.
Mott, N. F. & Devis, E. A. (1979). *Electron Processes in Non-crystalline Materials*. Oxford: Claredon Press.
Oxford Diffraction Ltd (2001). *Xcalibur CCD System, CrysAlis Software System*, Version 1.166. Oxford, England.
Petricek, V. & Dusek, M. (2000*a*). *JANA*2000, α Version. Institute of Physics, Academy of Sciences of the Czech Republic, Prague, Czech Republic.
Petricek, V. & Dusek, M. (2000*b*). *JANA*2000, β Version. Institute of Physics, Academy of Sciences of the Czech Republic, Prague, Czech Republic.
Restori, R. & Schwarzenbach, D. (1996). *Acta Cryst.* A**52**, 369–378.
Wiseman, P. J. & Dickens, P. (1976). *J. Solid State Chem.* **17**, 91–100.
Zhurova, E. A., Zavodnik, V. E., Ivanov, S. A., Syrnikov, P. P. & Tsirelson, V. G. (1992). *Russ. J. Inorg. Chem.* **37**, 1240–1244.
Zhurova, E. A., Zavodnik, V. E. & Tsirelson, V. G. (1995). *Crystallogr. Rep.* **40**, 816–823.